





## Light-induced rearrangement from macrocyclic to bicyclic lactam: A case study of *N*-chlorinated lauro lactam

### ABSTRACT

GABRIJEL ZUBČIĆ<sup>1</sup>   
KRISTINA PAVIĆ<sup>1</sup>   
JIANGYANG YOU<sup>2</sup>   
VALERIJE VRČEK<sup>1</sup>   
TOMISLAV PORTADA<sup>2</sup>   
ERIM BEŠIĆ<sup>1</sup>   
DAVOR ŠAKIĆ<sup>1,\*</sup> 

<sup>1</sup> University of Zagreb Faculty  
of Pharmacy and Biochemistry  
10 000 Zagreb, Croatia

<sup>2</sup> Ruđer Bošković Institute  
10 000 Zagreb, Croatia

Converting macrocycle lactams into bicyclic lactams is proposed as an additional way to further increase the metabolic stability of peptide-based drugs. Unfortunately, the synthesis of bicyclic lactams has to start almost from scratch. This study explores the Hofmann-Löffler-Freytag (HLF) reaction mechanism and products as a potential late-stage functionalisation strategy for facile conversion of macrocyclic to bicyclic ring. Lauro lactam, a macrocyclic amide, exhibits significant potential for transformation into bioactive bicyclic structures with smaller,  $\beta$ -,  $\gamma$ -,  $\delta$ -, and  $\epsilon$ -lactam rings, further increasing rigidity and hydrolytic stability. With irradiation provided by a 370 nm lamp, light-induced rearrangement reaction was monitored using nuclear magnetic resonance (NMR), while involved radical intermediates were trapped using *N*-tert-butyl- $\alpha$ -phenylnitron (PBN) spin-trap and characterised *via* EPR. While only two radical adduct types were identified in the electron paramagnetic resonance (EPR) (C-centered radical and chlorine radical), all eight possible products are observed in the NMR. Quantum chemical calculations provide deeper insights into reaction thermodynamics and kinetics, explaining why the *N*-centered radical was not observed. This research highlights the feasibility of using the HLF reaction to transform macrocyclic lactams into stable bicyclic drug candidates, paving the way for new therapeutic developments.

Accepted September 14, 2024  
Published online September 15, 2024

**Keywords:** radical rearrangement, radical thermodynamics, ring-contraction, late-stage functionalisation, synthetic strategy

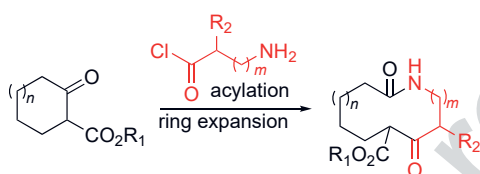
### INTRODUCTION

Late-stage functionalisation (LSF) has emerged as a transformative strategy in medicinal chemistry, providing powerful means to generate new potential drugs from existing lead compounds. This approach involves the modification of complex molecules at a late synthetic stage, allowing for the introduction of diverse functional groups without the need for extensive synthetic reroutes. By enabling the fine-tuning of pharmacological

\* Correspondence; e-mail: davor.sakic@pharma.unizg.hr

properties such as potency, selectivity, and metabolic stability, LSF plays a crucial role in optimising lead compounds and accelerating the drug development process (1, 2).

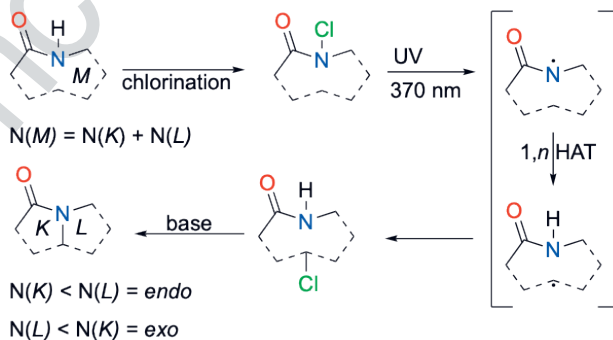
Among the "reaction toolbox" for LSF are ring-expansion reactions, which are particularly valuable for synthesising medium-sized and macrocyclic rings (3). These large-ring frameworks are critical in medicinal chemistry, with many drugs based on these structures on the market. The ability to create and modify these ring systems through LSF enables the development of drug candidates with unique structural and functional properties (4).



Scheme 1. Example of ring expansion in the late-stage functionalisation protocols. Adapted from reference (3).

Among macrocyclic drugs, a special place is reserved for lactams, as some of the most significant heterocycles in a variety of natural products and drugs, including antimicrobial drugs. Lactams as cyclic amides are classified by ring size, including four-membered ( $\beta$ -lactams, 2-azetidinones), five-membered ( $\gamma$ -lactams, 2-pyrrolidinones), six-membered ( $\delta$ -lactams, 2-piperidinones), seven-membered ( $\epsilon$ -lactams, 2-azepanones), medium-sized (8–11-membered), and macrocyclic ( $\geq 12$ -membered) rings. Moreover, lactams serve as conformationally restricted scaffolds that enhance the potency, selectivity, and metabolic stability of peptide-based drugs. They exhibit a broad spectrum of biological activities, making them valuable in the treatment of cancer, diabetes, infectious diseases, and more (5).

Changing macrocyclic lactams to bicyclic lactams with smaller ring motifs, such as  $\beta$ -,  $\gamma$ -,  $\delta$ , and  $\epsilon$ -lactams, may provide new opportunities for drug development. To make a ring contraction, a previously unfunctionalized C–H bond has to be activated to form a novel C–N bond (6). The photocatalytic Hofmann-Löffler-Freytag (HLF) reaction (7–11) is a



Scheme 2. Example of ring-contraction using Hofmann-Löffler-Freytag reaction.

promising method for achieving this transformation and has been used in alkaloid synthesis (12, 13). It employs *N*-centered radicals to functionalise remote C–H bonds. Our recent investigations into the mechanistic details of the HLF reaction have provided insights into its utility in synthesising nicotine derivatives in a cost-effective way while conserving stereoconfiguration (14). The cause of regioselectivity in the HLF reaction, where more pyrrolidine than piperidine products are formed, has recently been explained, and that could steer in producing only select bicyclic structures in the macrocycle (15).

In this study, we aim to modify laulolactam (azacyclotridecan-2-one, dodecalactam), which is industrially utilised as a monomer in the polymerisation of nylon-12, to serve as a model compound and potential scaffold for further bicyclic lactam synthesis. By leveraging the HLF reaction, we intend to demonstrate the feasibility of this approach, paving the way for the development of new, stable bicyclic drug candidates from macrocyclic leads.

## EXPERIMENTAL

### General

The purchased compounds were sourced from Sigma-Aldrich (USA) (azacyclotridecan-2-one, trichloroisocyanuric acid (TCICA), Celite® S), Fisher Scientific (USA) (dichloromethane, DCM) and Kemika (Croatia) (sodium hydroxide). All chemicals and solvents were obtained commercially and used without further purification unless otherwise noted.

Reactions were routinely checked by thin-layer chromatography (TLC) with Merck silica gel 60F-254 glass plates (Merck, Germany) using cyclohexane/ethyl acetate/methanol 3:1:0.5 as a solvent system. Spots were visualized by spraying the TLC plates with an ethanolic solution of phosphomolybdic acid followed by heating.

Photocatalysed reactions were performed *in situ* (reaction of **1-Cl** and EPR studies) and *off-site* (NMR) with Kessil PR-160L 370 ± 10 nm gen-2 LED UV (DiCon, USA), with an average intensity of 137 mW cm<sup>-2</sup> when the sample is at a 6-cm distance from the lamp, according to the manufacturer (16).

### Syntheses

#### *1-Chloroazacyclotridecan-2-one (1-Cl)*

TCICA (0.561 g, 2.414 mmol) was added to a stirred solution of azacyclotridecan-2-one (**1**) (0.433 g, 2.194 mmol) in DCM (17 mL) at 0 °C. The reaction mixture was stirred overnight at room temperature. The mixture was filtered through Celite® and the filtrate evaporated under reduced pressure to give the *N*-chloro derivative (0.488 g, 96 %).

### Cyclisation

After one-hour long irradiation of **1-Cl** using a 370 nm lamp in the round-bottom flask, while checking the reaction progress with TLC, the reaction was quenched with an excess of 0.1 mol L<sup>-1</sup> solution of NaOH. Products were filtrate evaporated under reduced pressure and washed with deionised water.

### *NMR and EPR reaction monitoring*

NMR spectra of the reaction mixture were obtained on a Varian Inova 400 NMR spectrometer (Varian, USA) operating at 399.90 MHz for  $^1\text{H}$  NMR and 100.6 MHz for  $^{13}\text{C}$  NMR. Chemical shifts ( $\delta$ ) are reported in parts per million (ppm). First,  $^1\text{H}$  and APT- $^{13}\text{C}$  spectra of the starting compound **1-Cl** were acquired. Then the sample was irradiated off-site for 5 minutes from the bottom of the NMR tube using the UV lamp at 25 % power. Reaction progress was monitored with  $^1\text{H}$  spectra, and for every three irradiation intervals, APT- $^{13}\text{C}$  was recorded. Deuterated chloroform was used as a solvent, with some precipitation forming during the reaction. Quenched and washed products were analysed in DMSO- $d_6$  solvent. The spectra were processed in the MNova 11.0.4 software (Mestrelab, Spain) (17) and using the NMRium online platform (Zakodium, Switzerland) (18).

EPR spectroscopy was done using a Bruker E500 ELEXSYS EPR spectrometer (Bruker, USA) with an ER4122SHQE cavity resonator. As this cavity resonator does not have an optical window for illumination, the light source was mounted underneath the cavity, with light coming through the bottom of the EPR 4 mm-inner-diameter tube, with toluene as a solvent. EPR deconvolution and simulation were done using an EasySpin module (19) with the MATLAB program package. (MATLAB, Natick, USA) EPR visualization and simulations were done using the VisualEPR Web page (20).

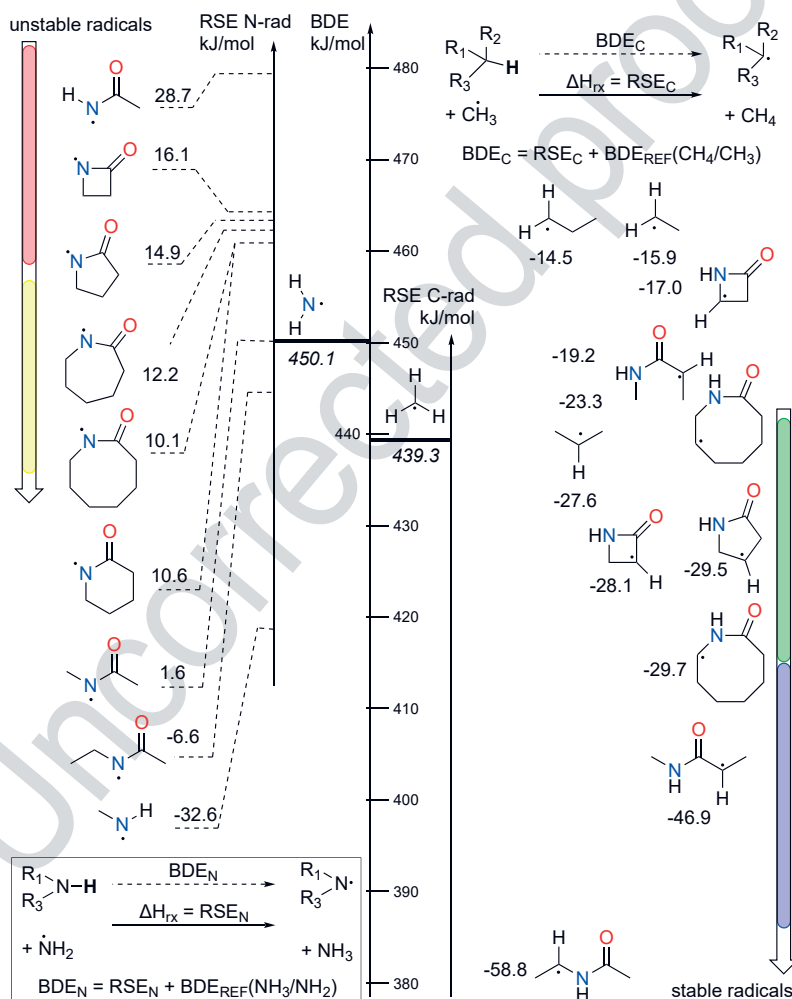
### *Computational methods*

Initial structures were optimised using the semi-empirical tight-binding quantum chemical method xtb program package (21). Conformational space for reactants, products, and transition states was sampled and investigated using the Conformer-Rotamer Ensemble Sampling Tool – CREST (22) coupled with meta-dynamic simulations (23) on the GFN2-xtb level of theory (24). Selected 50 lowest energy conformations were re-optimised using density functional theory on B3LYP/6-31G(d) level of theory (25, 26) using Gaussian 16 program package (27). For each structure, frequency calculation was performed to identify if the structure is a minimum or a saddle point (minimum in all directions except in one path, identifying transition-state structure) on the potential energy surface. From the transition-state structure, an intrinsic reaction coordinate search was performed to characterise the corresponding reaction and product complexes/reactive conformers. All conformer ensembles were sorted via the CREGEN procedure, and improved energetics were obtained *via* single-point calculations using RO-B2PLYP-D3/G3MP2Large level of theory (28–31). Calculations were performed using the advanced computing service (cluster Supek) provided by the University of Zagreb University Computing Centre – SRCE (32) and the computational resources of the PharmInova project (sw.pharma.hr) at the University of Zagreb Faculty of Pharmacy and Biochemistry (33), and all visualisations were done using IQmol (34).

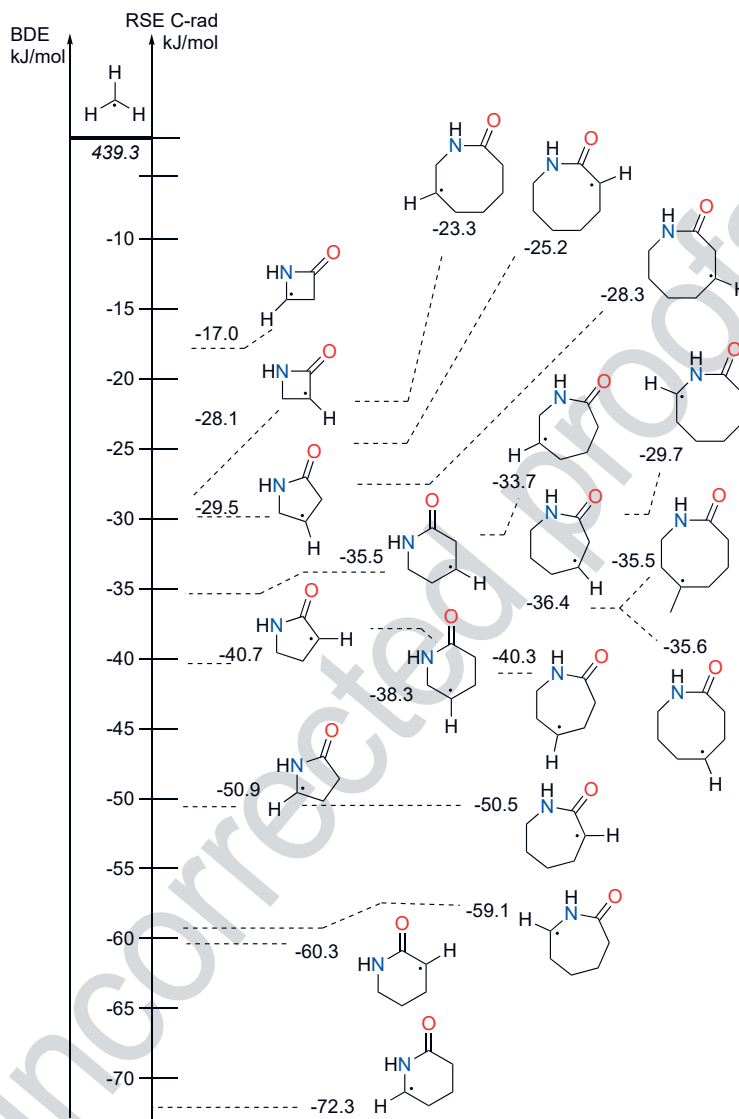
## RESULTS AND DISCUSSION

HLF reaction is governed by the thermodynamic factors, namely the difference in the radical stability between reactants and products in the rate-determining step (35). A well-proven method used for the calculation and prediction of radical stabilities among the

*N*-centered and *C*-centered radicals is done *via* modelling of isodesmic reactions involving one experimentally well-defined standard. For *C*-centered radicals, the standard is methane/methyl radical, while for *N*-centered radicals ammonia/aminyl radical is used as an anchor point, with bond-dissociation energies (BDEs) of  $439.3 \pm 0.4 \text{ kJ mol}^{-1}$  and  $450.1 \pm 0.24 \text{ kJ mol}^{-1}$ , respectively (36). Reaction enthalpy of such isodesmic reactions is called radical stabilisation energy (RSE) and can be used to gauge the relative difference between the same class of radicals, but also a good approximation of BDE, when added to the referent BDE. In Scheme 3, different relevant *N*-centered and *C*-centered radicals present in lactams and similar compounds (amidyl, aminyl, and alkyl radicals) are shown. A clear effect of sterical influence on the stability of amidyl radicals can be observed. Namely, for *N*-methyl-acetamide



Scheme 3. BDE/RSE of selected *N*-centered radicals and *C*-centered radicals.



Scheme 4. BDE/RSE of C-centered radicals in lactam structures.

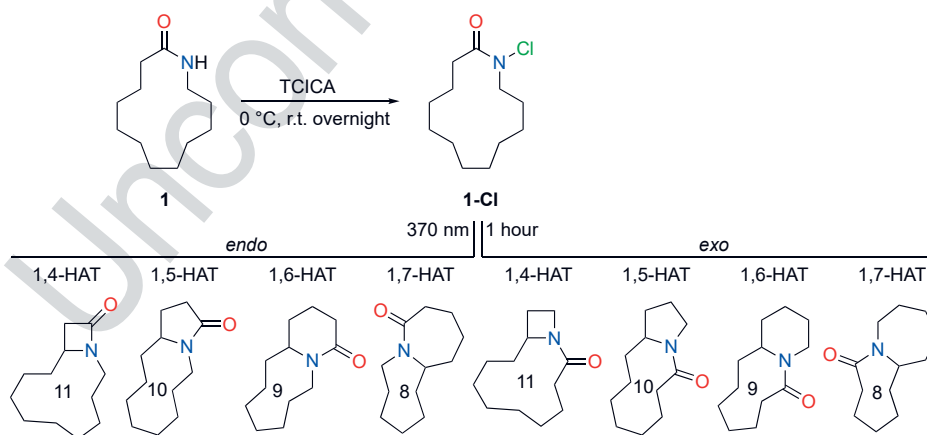
amidyl radical, RSE is  $1.6 \text{ kJ mol}^{-1}$ , but when constricted in 2-azetidinone, 2-pyrrolidinone, 2-peperidinone, 2-azepanone, and 2-azocanone less stable amidyl radicals are formed, with RSEs in the range of  $10.1$  to  $16.1 \text{ kJ mol}^{-1}$ . But as the ring grows, the structural effect on the radical is less pronounced, and for lauro lactam amidyl radical (**1-Nrad**), RSE of  $-1.9 \text{ kJ mol}^{-1}$  is between radical stability of *N*-methyl and *N*-ethyl ( $\text{RSE} = -6.6 \text{ kJ mol}^{-1}$ ) derivatives of acetamide.

C-centered radicals are generally more stable than *N*-centered amidyl radicals (see Schemes 3 and 4). Alkyl radicals have RSE around that of C<sub>2</sub>-radical in propane (−27.6 kJ mol<sup>−1</sup>), ranging from −23.3 kJ mol<sup>−1</sup> in C<sub>7</sub>-radical of 2-azocanone to −40.3 kJ mol<sup>−1</sup> in C<sub>5</sub>-radical of 2-azepanone. While alkyl radicals surrounded by methylene neighbours are in the aforementioned range, C-centered radicals with carbonyl or amine part of amide next to it are more stable. The exceptions to that rule are radicals in β-lactam (2-azetidione), which are heavily constrained and are among the least stable C-centered radicals, comparable only to the primary radicals.

From Schemes 3 and 4 it is obvious that the HLF reaction is exothermic in the radical rearrangement reaction, and can occur in lactam rings of various sizes.

Next, we wanted to test our theory on a real macrocyclic lactam, specifically on lauro lactam, in order to model all transition states and products stemming from the HLF reaction. The first step of the HLF reaction is light-induced homolytic cleavage of the *N*-halogen bond. To that end, an *N*-chloro derivative (**1-Cl**) of lauro lactam (**1**) was prepared by *N*-chlorination with TCICA (Scheme 5).

Quantum-chemical methods were used to model all transition states and all products stemming from the HLF reaction. Possible 1,*n*-HAT reactions include 1,4-HAT, 1,5-HAT, 1,6-HAT, and 1,7-HAT forming 4-, 5-, 6-, and 7-membered rings, respectively (see Scheme 5). However, there are two different ways to form those rings. One pathway generates the product with the carbonyl group inside the smaller, newly formed ring, titled *endo*. Consequently, newly formed rings with the carbonyl group outside the smaller ring are termed *exo*. In Table I, calculated parameters are presented for all combinations. The lowest barriers ( $\Delta H_{298}^\ddagger$ ) are present in the *exo*-1,5-HAT and *exo*-1,6-HAT for the cyclisation. The *endo*-1,5-HAT process is more stable than both *endo*-1,6-HAT and *endo*-1,7-HAT for *endo*-type of cyclisation, and very similarly stable to the 1,7-HAT path of *exo*-type. To our surprise, the barrier for the *endo*-1,4-HAT reaction is lower than the *exo*-1,4-HAT reaction. The formation of the β-lactam ring by 1,4-HAT *endo*-type of cyclisation is two orders of magnitude



Scheme 5. *N*-chlorination of lauro lactam and tentative products after 1-hour irradiation with 370 nm lamp.

Table I. Calculated reaction parameters in the 1,*n*-HAT rearrangement reactions between amidyl *N*-centered and *C*-centered radicals.<sup>a</sup>

1, <i>n</i> -HAT	exo		endo	
	$\Delta H_{rx,298}$ (kJ mol <sup>-1</sup> )	$\Delta H_{298}^\ddagger$ (kJ mol <sup>-1</sup> )	$\Delta H_{rx,298}$ (kJ mol <sup>-1</sup> )	$\Delta H_{298}^\ddagger$ (kJ mol <sup>-1</sup> )
1,4-HAT	-38.38	61.41	-36.89	45.38
	azetidine		β-lactam	
1,5-HAT	-37.86	25.26	-33.37	32.13
	pyrrolidine/azolidine		γ-lactam	
1,6-HAT	-41.31	25.40	-40.28	35.04
	piperidine		δ-lactam	
1,7-HAT	-41.90	33.13	-41.27	34.56
	azepine		ε-lactam	

<sup>a</sup> The bottom row describes the formed ring in the subsequent reaction with the base.

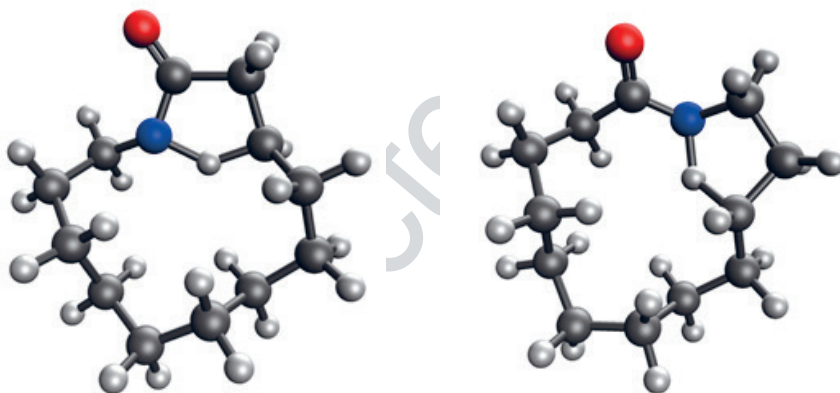


Fig. 1. Transition-state structures for *endo*-1,4-HAT and *exo*-1,4-HAT

faster than the formation of azetidone by the *exo*-1,4-HAT, as seen from the calculated rate constants for *endo*- ( $k_{endo-1,4-HAT} = 6.899 \times 10^4 \text{ s}^{-1}$ ) and *exo*- ( $k_{exo-1,4-HAT} = 1.069 \times 10^2 \text{ s}^{-1}$ ) pathways of 4-membered ring cyclisations (transition-state structures are shown in Fig. 1). The stabilities of all products are similar and provide a strong thermodynamic force (reaction enthalpy,  $\Delta H_{rx,298}$ ) towards products.

Next, EPR experiments were performed as described in the method section. After spectra deconvolution, only two different radicals are observed. The major observed radical is the adduct of chlorine radical onto the *N*-*tert*-butyl- $\alpha$ -phenylnitron (PBN), **CI-PBN**, with hyperfine splitting constant (*hfc*)  $A_N = 12.36 \text{ G}$ ,  $A_H = 0.75 \text{ G}$  and  $A_H = 6.22 \text{ G}$ , with a line width of 0.22. Another radical is a *C*-centered radical adduct of PBN, **C-PBN**, with a difference in *g*-value of  $-0.0013$  from **CI-PBN**, and *hfc*  $A_N = 13.44 \text{ G}$ ,  $A_H = 1.76 \text{ G}$ . After decomposition, some residual signals remain with some weak and broad components which are



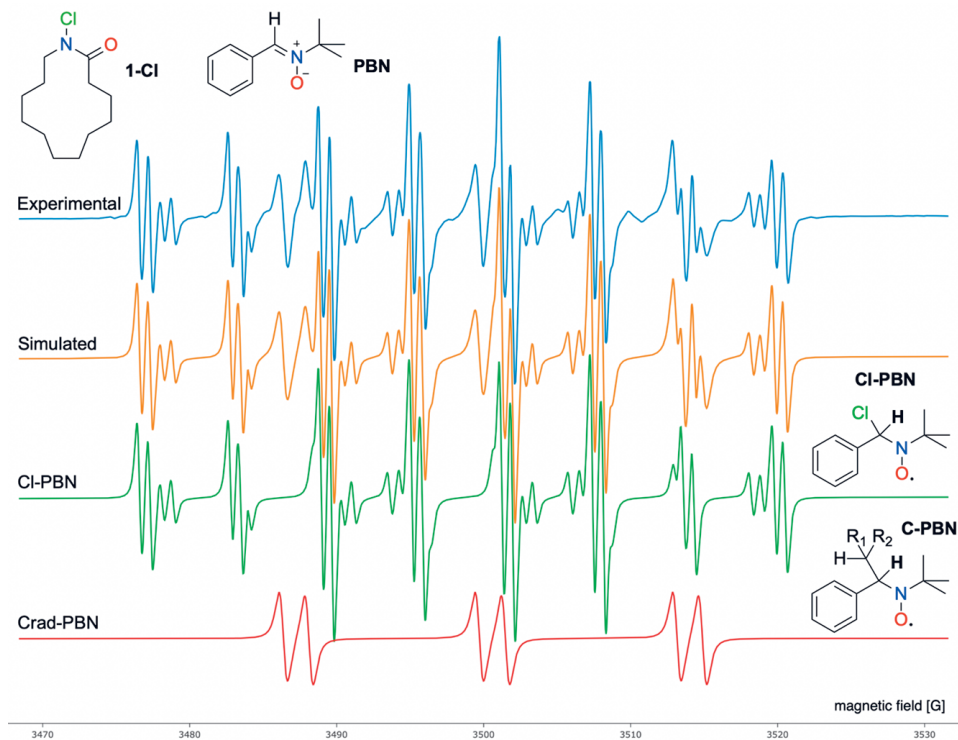


Fig. 2. EPR spectra of spin-trapped radical intermediates generated with a 370 nm irradiation of **1-Cl**. The experimental spectrum is in blue, while red, green, and orange correspond to simulated spectra for **Crad-PBN**, **Cl-PBN**, and total simulated spectra, respectively.

similar to the **N-PBN** adduct radical observed in our previous work (15). Yet the residue signal is extremely weak, making it difficult to achieve a satisfactory deconvolution. Since the reactions happen very quickly, the rearrangement of *N*-centered radical to the *C*-centered radicals occurs faster than the spin-trapping reaction of PBN.

Finally, NMR experiments were performed to identify the reaction products. The biggest obstacle encountered in the NMR experiments was the relative insolubility of the compound **1-Cl** and its products in  $\text{CDCl}_3$  solvent. As the reaction progressed, precipitation was formed in the NMR tube, making prolonged spectra acquisition unfeasible. To address this issue, the photoreaction was quenched with  $0.1 \text{ mol L}^{-1}$  NaOH (added in excess), washed with water, and then 30 mg of the product mixture was resuspended in  $\text{DMSO-}d_6$  for NMR spectroscopy. In Fig. 3, APT- $^{13}\text{C}$  NMR spectra are shown, along with an enlarged portion of the spectra displaying signals of carbon atoms with an odd number of attached H-atoms. In the spectra, nine such signals can be observed, with a dubious signal at 62.05 ppm. If we disregard that signal, eight different signals actually correspond to the eight different products predicted *via* calculations (see Scheme 5).

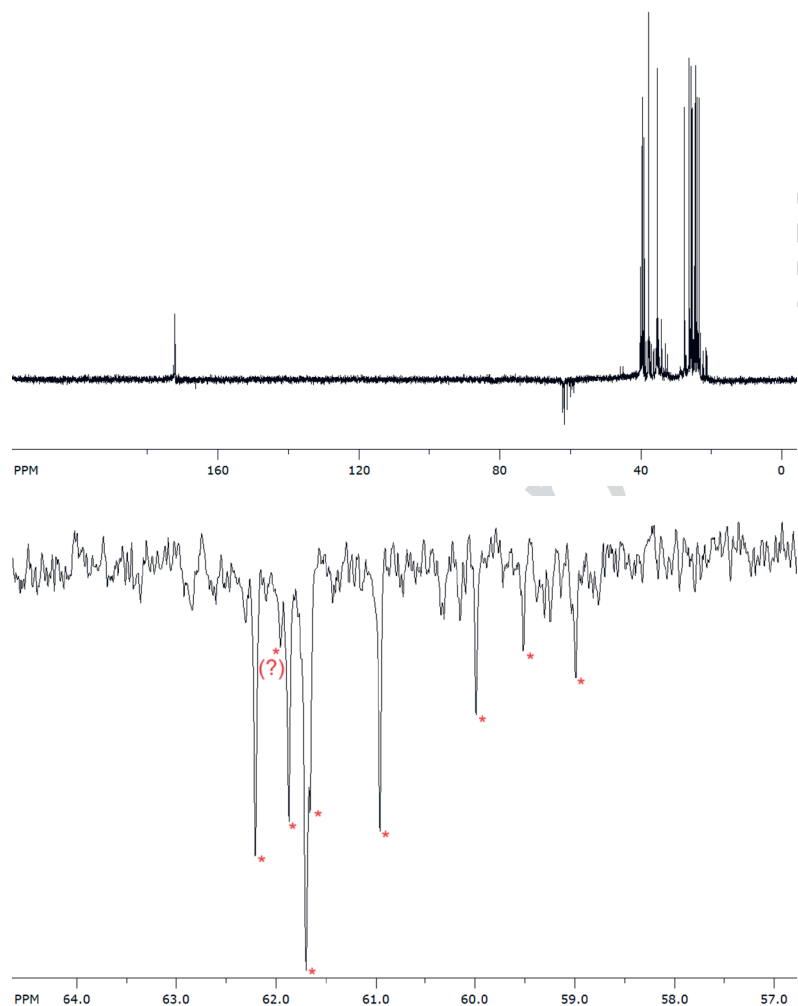


Fig. 3. a) APT-<sup>13</sup>C NMR spectra of the quenched and washed reaction; b) eight different signals in the negative region from 57–64 ppm correspond to eight different products.

Thus, we have demonstrated that HLF reaction can be used in the LSF strategies to produce all types of bicyclic rings from lactam macrocycles, with ring sizes ranging from 4-membered rings, up to 7-membered rings.

## CONCLUSIONS

This study successfully demonstrates the potential of the Hofmann-Löffler-Freytag (HLF) reaction as a viable method for late-stage functionalization (LSF) of macrocyclic lactams, as shown with lauro lactam. The thermodynamically driven HLF reaction, char-

acterised by radical stability differences, effectively transforms lauro lactam into various bicyclic lactams with ring sizes ranging from 4- to 7-membered rings. These transformations, investigated with theoretical and experimental approaches, underscore the versatility and efficiency of the HLF reaction in generating structurally diverse and stable products. Amidyl radicals in constrained lactam rings exhibit higher radical stabilization energy (RSE) values, indicating reduced stability. C-centered radicals, particularly those adjacent to carbonyl or amine groups, demonstrate enhanced radical stability, with notable exceptions in highly constrained structures like 2-azetidinone. Computational modelling reveals the lowest activation barriers for 1,5- and 1,6-HAT *exo*-type cyclizations with carbonyl moiety outside the smaller ring. The unexpected lower barrier for 1,4-HAT *endo*-type reactions compared to *exo*-type counterparts highlights the complexity and potential of the HLF mechanism in the formation of pharmacologically potent  $\beta$ -lactam motif. EPR spectroscopy identifies **CI-PBN** and **C-PBN** as primary radical adducts to the spin-trap *N*-*tert*-butyl- $\alpha$ -phenylnitron (PBN), underpinning rapid *N*- to C-centered radical rearrangement. NMR spectroscopy confirms the formation of eight distinct products, aligning with computational predictions. The findings affirm the HLF reaction's applicability in LSF strategies, enabling the production of various bicyclic rings from macrocyclic lactams. This approach not only broadens the scope of accessible ring structures but also facilitates the fine-tuning of pharmacological properties, crucial for drug development. Future research should focus on exploring different macrocyclic substrates, optimising reaction conditions, and conducting biological evaluations to fully harness the HLF reaction's potential in drug development.

*Abbreviations, acronyms, symbols.* – APT, attached proton test; BDE, bond dissociation energy; EPR, electron paramagnetic resonance;  $\Delta H^\ddagger_{298}$ , activation enthalpy at 298K;  $\Delta H_{rx,298}$ , reaction enthalpy at 298K; HAT, hydrogen atom transfer; hfc, hyperfine coupling constant; HLF, Hofmann-Löffler-Freytag; LED UV, light-emitting diode in ultraviolet radiation; LSF, late-stage functionalization; NMR, nuclear magnetic resonance; PBN, *N*-*tert*-butyl- $\alpha$ -phenylnitron; RSE, radical stabilization energy; TCICA, trichloroisocyanuric acid.

*Acknowledgments.* – The authors would like to acknowledge financial support from the Croatian Science Foundation Installation grant UIP-2020-02-4857 LIGHT-N-RING, grant IP-2022-10-2634 PharmaEco, and computational resources available on Cluster Supek, EU funded through KK.01.1.1.08.0001, a part of the Advanced Computing Service provided by University of Zagreb University Computing Centre – SRCE. This work was also supported by the project FarmInova at the Faculty of Pharmacy and Biochemistry University of Zagreb (KK.01.1.1.02.0021) funded by the European Regional Development Fund. Support from The Cryogenic Centre at the Institute of Physics project (KaCIF, KK.01.1.1.02.0012) is acknowledged.

*Funding.* – This research received no external funding.

*Conflicts of interest.* – The authors declare no conflict of interest.

*Authors contributions.* – Conceptualization, D.Š. and G.Z.; calculations, data analysis, G.Z.; methodology, experimental, J.Y., K.P. and T.P.; analysis, T.P. and V.V.; writing, original draft preparation, D.Š.; writing, review and editing, E.B. and D.Š.; funding, D.Š. All authors have read and agreed to the published version of the manuscript.

## REFERENCES

1. T. Cernak, K. D. Dykstra, S. Tyagarajan, P. Vachal and S. W. Krska, The medicinal chemist's toolbox for late stage functionalization of drug-like molecules, *Chem. Soc. Rev.* 45(3) (2016) 546–576; <https://doi.org/10.1039/C5CS00628G>

2. S. K. Sinha, S. Guin, S. Maiti, J. P. Biswas, S. Porey and D. Maiti, Toolbox for distal C–H bond functionalizations in organic molecules, *Chem. Rev.* **122**(6) (2022) 5682–5841; <https://doi.org/10.1021/acs.chemrev.1c00220>
3. Z. Yang, M. Arnoux, D. Hazelard, O. R. Hughes, J. Nabarro, A. C. Whitwood, M. A. Fascione, C. D. Spicer, P. Compain and W. P. Unsworth, Expanding the scope of the successive ring expansion strategy for macrocycle and medium-sized ring synthesis: unreactive and reactive lactams, *Org. Biomol. Chem.* **22** (2024) 2985–2991; <https://doi.org/10.1039/D4OB00285G>
4. L. G. Baud, M. A. Manning, H. L. Arkless, T. C. Stephens and W. P. Unsworth, Ring-expansion approach to medium-sized lactams and analysis of their medicinal lead-like properties, *Chem. Eur. J.* **23** (2017) 2225–2230; <https://doi.org/10.1002/chem.201605615>
5. F. I. Saldívar-González, E. Lenci, A. Trabocchi and J. L. Medina-Franco, Exploring the chemical space and the bioactivity profile of lactams: a chemoinformatic study, *RSC Adv.* **9** (2019) Article ID 27105 (12 pages); <https://doi.org/10.1039/c9ra04841c>
6. P. Bellotti, H.-M. Huang, T. Faber and F. Glorius, Photocatalytic late-stage C–H functionalization, *Chem. Rev.* **123**(8) (2023) 4237–4352; <https://doi.org/10.1021/acs.chemrev.2c00478>
7. A. W. Hofmann, Ueber die Einwirkung des Broms in alkalischer Lösung auf die Amine, *Ber. Dtsch. Chem. Ges.* **16**(1) (1883) 558–560; <https://doi.org/10.1002/cber.188301601120>
8. A. W. Hofmann, Ueber die Einwirkung des Broms in alkalischer Lösung auf Amide, *Ber. Dtsch. Chem. Ges.* **14**(2) (1881) 2725–2736; <https://doi.org/10.1002/cber.188101402242>
9. A. W. Hofmann, Zur Kenntniss der Coniin-Gruppe, *Ber. Dtsch. Chem. Ges.* **18**(1) (1885) 109–131; <https://doi.org/10.1002/cber.18850180126>
10. K. Löffler and C. Freytag, Über eine neue Bildungsweise von *N*-alkylierten Pyrrolidinen, *Ber. Dtsch. Chem. Ges.* **42**(3) (1909) 3427–3431; <https://doi.org/10.1002/cber.19090420377>
11. G. Zubčić, S. Shkunnikova, D. Šakić and M. Marijan, Renaissance of Hofmann-Löffler-Freytag reaction – Development of C–H functionalisation strategies based on green chemistry principles, *Kem. Ind.* **71**(5–6) (2022) 359–373; <https://doi.org/10.15255/KUI.2021.070>
12. S. W. Baldwin and R. J. Doll, Synthesis of the 2-aza-7-oxatricyclo[4.3.2.0<sup>4,8</sup>]undecane nucleus of some gelsemium alkaloids, *Tetrahedron Lett.* **20**(35) (1979) 3275–3278; [https://doi.org/10.1016/S0040-4039\(01\)95450-2](https://doi.org/10.1016/S0040-4039(01)95450-2)
13. K. Löffler and S. Kober, Über die Bildung desi-Nicotins aus *N*-Methyl-*p*-pyridyl-butylamin (Dihydrometanicotin), *Ber. Dtsch. Chem. Ges.* **42** (1909) 3431–3438; <https://doi.org/10.1002/cber.19090420378>
14. S. Shkunnikova, H. Zipse and D. Šakić, Role of substituents in the Hofmann-Löffler-Freytag reaction. A quantum-chemical case study on nicotine synthesis, *Org. Biomol. Chem.* **19** (2021) 854–865; <https://doi.org/10.1039/D0OB02187C>
15. G. Zubčić, J. You, F. L. Zott, S. S. Ashirbaev, M. K. Marković, E. Bešić, V. Vrček, H. Zipse and D. Šakić, Regioselective rearrangement of nitrogen- and carbon-centered radical intermediates in the Hofmann-Löffler-Freytag reaction, *J. Phys. Chem. A* **128**(13) (2024) 2574–2583; <https://doi.org/10.1021/acs.jpca.3c07892>
16. Kessil PR-160L 370-Gen2 specification; [https://www.kessil.com/products/science\\_PR160L.php](https://www.kessil.com/products/science_PR160L.php); last accessed date June 28, 2024.
17. M. R. Willcott, MestRe Nova, *J. Am. Chem. Soc.* **131**(36) (2009) 13180; <https://doi.org/10.1021/ja906709t>
18. L. Patiny, H. Musallam, A. Bolaños, M. Zasso, J. Wist, M. Karayilan, E. Ziegler, J. C. Liermann and N. E. Schlörer, NMRium: Teaching nuclear magnetic resonance spectra interpretation in an online platform, *Beilstein J. Org. Chem.* **20** (2024) 25–31; <https://doi.org/10.3762/bjoc.20.4>
19. S. Stoll and A. Schweiger, EasySpin, a comprehensive software package for spectral simulation and analysis in EPR, *J. Magn. Reson.* **178**(1) (2006) 42–55; <https://doi.org/10.1016/j.jmr.2005.08.013>
20. D. Šakić, G. Zubčić, J. You, T. Weitner, V. Chechik and E. Bešić, VisualEPR; <https://github.com/DSa-kicLab/visualEPR>; last accessed date December 1, 2023.

21. C. Bannwarth, E. Caldeweyher, S. Ehlert, A. Hansen, P. Pracht, J. Seibert, S. Spicher and S. Grimme, *WIREs Comput. Mol. Sci.* **11** (2020) Article ID e01493 (49 pages); <https://doi.org/10.1002/wcms.1493>
22. P. Pracht, F. Bohle and S. Grimme, Automated exploration of the low-energy chemical space with fast quantum chemical methods, *Phys. Chem. Chem. Phys.* **22** (2020) 7169–7192; <https://doi.org/10.1039/C9CP06869D>
23. S. Grimme, Exploration of chemical compound, conformer, and reaction space with meta-dynamics simulations based on tight-binding quantum chemical calculations, *J. Chem. Theory Comput.* **15**(5) (2019) 2847–2862; <https://doi.org/10.1021/acs.jctc.9b00143>
24. C. Bannwarth, S. Ehlert and S. Grimme, GFN2-xTB – An accurate and broadly parametrized self-consistent tight-binding quantum chemical method with multipole electrostatics and density-dependent dispersion contributions, *J. Chem. Theory Comput.* **15**(3) (2019) 1652–1671; <https://doi.org/10.1021/acs.jctc.8b01176>
25. A. D. Becke, Density-functional thermochemistry. III. The role of exact exchange, *J. Chem. Phys.* **98**(7) (1993) 5648–5652; <https://doi.org/10.1063/1.464913>
26. R. Ditchfield, W. J. Hehre and J. A. Pople, Self-consistent molecular-orbital methods. IX. An extended gaussian-type basis for molecular-orbital studies of organic molecules, *J. Chem. Phys.* **54**(2) (1971) 724–728; <https://doi.org/10.1063/1.1674902>
27. M. J. Frisch, G. W. Trucks, H. B. Schlegel, G. E. Scuseria, M. A. Robb, J. R. Cheeseman, G. Scalmani, V. Barone, G. A. Petersson, H. Nakatsuji, X. Li, M. Caricato, A. V. Marenich, J. Bloino, B. G. Janesko, R. Gomperts, B. Mennucci, H. P. Hratchian, J. V. Ortiz, A. F. Izmaylov, J. L. Sonnenberg, D. Williams-Young, F. Ding, F. Lipparini, F. Egidi, J. Goings, B. Peng, A. Petrone, T. Henderson, D. Ranasinghe, V. G. Zakrzewski, J. Gao, N. Rega, G. Zheng, W. Liang, M. Hada, M. Ehara, K. Toyota, R. Fukuda, J. Hasegawa, M. Ishida, T. Nakajima, Y. Honda, O. Kitao, H. Nakai, T. Vreven, K. Throssell, J. A. Montgomery, Jr., J. E. Peralta, F. Ogliaro, M. J. Bearpark, J. J. Heyd, E. N. Brothers, K. N. Kudin, V. N. Staroverov, T. A. Keith, R. Kobayashi, J. Normand, K. Raghavachari, A. P. Rendell, J. C. Burant, S. S. Iyengar, J. Tomasi, M. Cossi, J. M. Millam, M. Klene, C. Adamo, R. Cammi, J. W. Ochterski, R. L. Martin, K. Morokuma, O. Farkas, J. B. Foresman and D. J. Fox. Gaussian 16. Wallingford CT, USA: Gaussian, Inc.; 2016.
28. S. Grimme, Semiempirical hybrid density functional with perturbative second-order correlation, *J. Chem. Phys.* **124**(3) (2006) Article ID 034108; <https://doi.org/10.1063/1.2148954>
29. S. Grimme, J. Antony, S. Ehrlich and H. Krieg, A consistent and accurate ab initio parametrization of density functional dispersion correction (DFT-D) for the 94 elements H-Pu, *J. Chem. Phys.* **132**(15) (2010) Article ID 154104; <https://doi.org/10.1063/1.3382344>
30. F. Neese, T. Schwabe and S. Grimme, Analytic derivatives for perturbatively corrected “double hybrid” density functionals: Theory, implementation, and applications, *J. Chem. Phys.* **126**(12) (2007) Article ID 124115; <https://doi.org/10.1063/1.2712433>
31. L. A. Curtiss, P. C. Redfern, K. Raghavachari, V. Rassolov and J. A. Pople, Gaussian-3 theory using reduced Møller-Plesset order, *J. Chem. Phys.* **110**(10) (1999) 4703–4709; <https://doi.org/10.1063/1.478385>
32. HR-ZOO, Cluster Supek; University of Zagreb University Computing Centre – SRCE, KK.01.1.1.08.0001, EU funded within OPCC for Republic of Croatia: Zagreb, 2023.
33. PharmInova Project, Cluster Sw.Pharma.Hr; University of Zagreb Faculty of Pharmacy and Biochemistry, KK.01.1.1.02.0021, EU funded by the European Regional Development Fund: Zagreb, 2023.
34. IQmol; <https://github.com/nutjunkie/IQmol>; last accessed date July 2, 2024.
35. D. Šakić and H. Zipse, Radical stability as a guideline in C–H amination reactions, *Adv. Synth. Catal.* **358** (2016) 3983–3991; <https://doi.org/10.1002/adsc.201600629>
36. Y.-R. Luo, *Comprehensive Handbook of Chemical Bond Energies*, CRC Press, London 2007.